NANO LETTERS

pubs.acs.org/NanoLett Letter

# Nanomechanics of CCN1-Mediated *Staphylococcus aureus* Phagocytosis

Can Wang, Telmo O. Paiva, Pietro Speziale,* and Yves F. Dufrêne*

Cite This: *Nano Lett.* 2024, 24, 8567−8574 Read Online

ACCESS | Metrics & More | Article Recommendations | Supporting Information



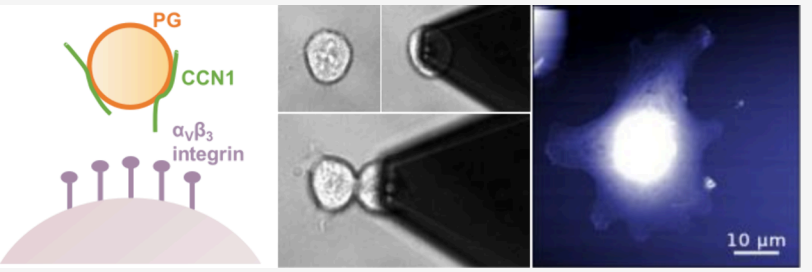


**ABSTRACT:** Phagocytosis is an essential mechanism of the human immune system where pathogens are eliminated by immune cells. The CCN1 protein plays an important role in the phagocytosis of *Staphylococcus aureus* by favoring the bridging of the $\alpha_V\beta_3$ integrin to the bacterial peptidoglycan (PG), through mechanical forces that remain unknown. Here, we employ single-molecule experiments to unravel the nanomechanics of the PG−CCN1−$\alpha_V\beta_3$ ternary complex. While CCN1 binds $\alpha_V\beta_3$ integrins with moderate force (∼60 pN), much higher binding strengths (up to ∼800 pN) are observed between CCN1 and PG. Notably, the strength of both CCN1−$\alpha_V\beta_3$ and CCN1−PG bonds is dramatically enhanced by tensile loading, favoring a model in which mechanical stress induces the exposure of cryptic integrin binding sites in CCN1 and multivalent binding between CCN1 lectin sites and monosaccharides along the PG glycan chains.

**KEYWORDS:** *single-molecule force spectroscopy, Staphylococcus aureus, phagocytosis, peptidoglycan, CCN1, $\alpha_V\beta_3$ integrin*

*Staphylococcus aureus* is a major human pathogen that causes many types of diseases, including infective endocarditis, osteomyelitis, sepsis, and metastatic infections.[1] This versatility arises from the ability of the bacteria to adhere to extracellular matrix and host cell surfaces components, facilitated by an array of surface-associated adhesion proteins, so-called microbial surface components recognizing adhesive matrix molecules (MSCRAMMs),[2] alongside lipoproteins and polysaccharides,[3,4] as well as secreted proteins such as exoenzymes and toxins.[5]

Peptidoglycan (PG) is a fundamental component of the bacterial cell wall that plays important roles in staphylococcal virulence. This enormous bag-shaped macromolecule consists of linear polysaccharide chains cross-linked by short peptide stems composed of alternating L- and D-amino acids. The polysaccharide chains are formed of alternating *N*-acetylglucosamine (GlcNAc) and *N*-acetylmuramic acid in $\beta$-1,4-glyosidic linkage.[6,7] Not only does PG confer structural integrity and protection against environmental stressors, but it also serves as a molecular pattern recognized by host innate immunity proteins,[8] including nucleotide-binding oligomerization domain (NOD)-like receptors,[9] toll-like receptors (TLRs),[10] and PG recognizing proteins (PGRPs).[11]

CCN1 (cysteine-rich 61, Cyr61) is the prototype of a secreted protein family produced by human fibroblasts and endothelial cells. Structurally, CCN1 consists of a secretory signal peptide (SP), an insulin-like growth factor binding domain (IGFBP), a von Willebrand type-C domain (vWC), a thrombospondin type-1 repeat (TSR) domain, and a cysteine knot motif in the C-terminal (CT) domain (Figure 1a).[12] CCN1 binds directly to specific integrin receptors in a cell type-specific manner, engaging co-receptors in some contexts.[13,14] This extracellular matrix-associated multifunctional protein regulates a broad spectrum of cellular activities, including cell adhesion, migration, proliferation, survival, and differentiation in embryonic development.[15] CCN1 is also present in the body fluids, playing a critical role in inflammation,[12,16] injury repair in the gut,[17] liver,[18] skin,[19] and cancer.[20] Besides, it can also regulate a set of genes that control angiogenesis and matrix remodeling,[21] and promote efferocytosis by binding to phosphatidylserine on the apoptotic cells. Bridging apoptotic neutrophils to macrophages via

**Received:** March 31, 2024
**Revised:** June 26, 2024
**Accepted:** June 26, 2024
**Published:** July 3, 2024

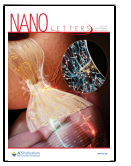





https://doi.org/10.1021/acs.nanolett.4c01533
*Nano Lett.* 2024, 24, 8567−8574

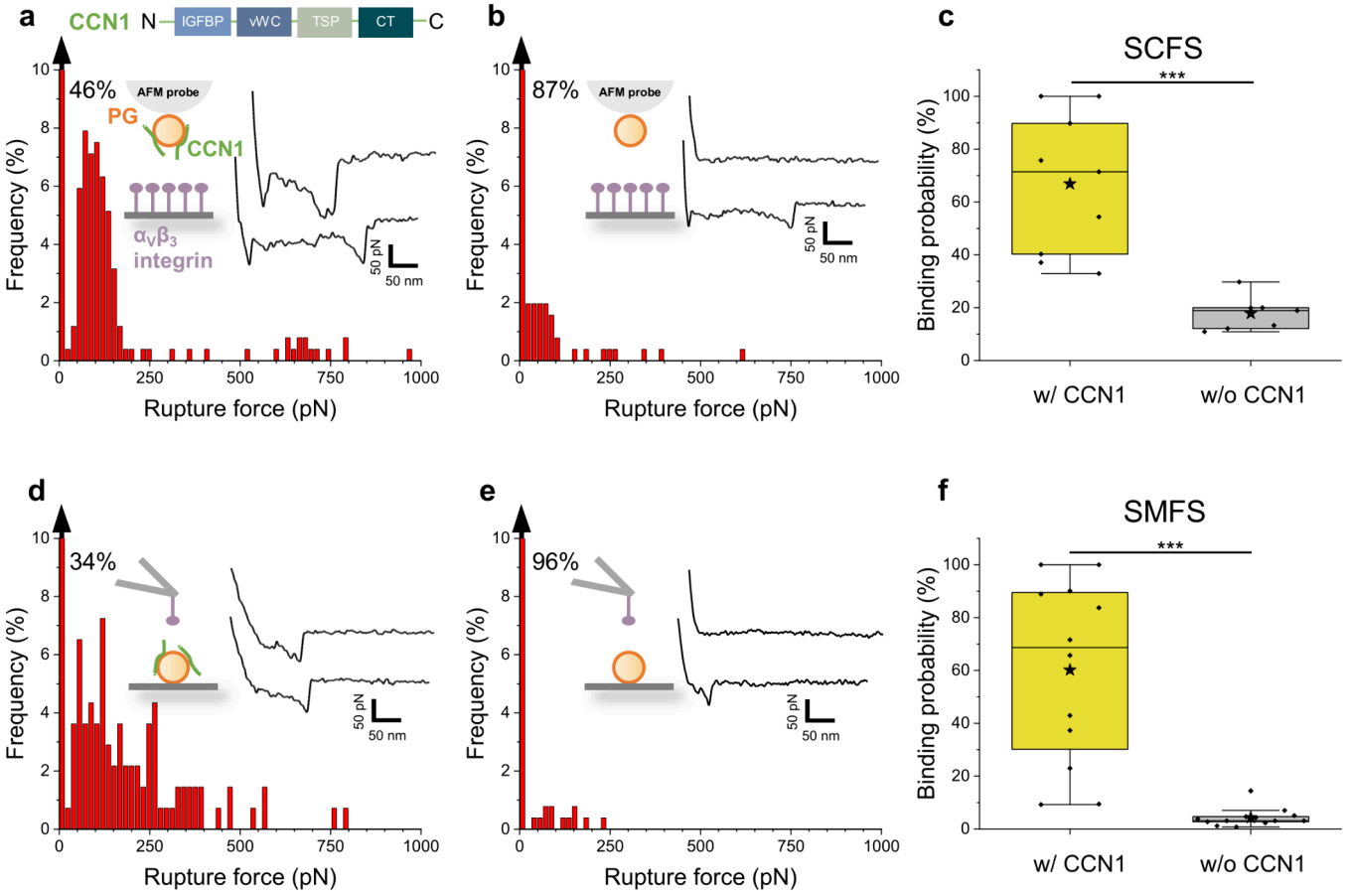


**Figure 1.** CCN1 promotes *S. aureus* adhesion to $\alpha_V\beta_3$ integrin. (a) Scheme for the CCN1 structure and representative rupture force histogram obtained by probing an $\alpha_V\beta_3$ integrin-functionalized surface with a single *S. aureus* cell preincubated with CCN1 using single cell force spectroscopy (SCFS). Treatment with CCN1 was performed statically at room temperature, for 1 h, at a final concentration of 50 $\mu$g mL$^{-1}$. For more cells, see Figure S1a. CCN1 binds *S. aureus* peptidoglycan (PG) and $\alpha_V\beta_3$ integrin through unknown mechanisms. It consists of four conserved domains with homologies to insulin-like growth factor-binding protein (IGFBP), von Willebrand factor type C repeat (vWC), thrombospondin type-1 repeat (TSR), and a cysteine-knot motif in the C-terminal (CT) domain. (b) Rupture force histogram of a representative native *S. aureus* cell, not treated with CCN1. For more cells, see Figure S1b. (c) Box plot showing the binding probability for *S. aureus cells* with or without CCN1 preincubation, measured by SCFS. $n$ = 9 and 7 cells, respectively. (d, e) Rupture force histograms of a single representative *S. aureus* cell treated (d) or not (e) by CCN1, probed with AFM tips functionalized with $\alpha_V\beta_3$ integrin using single molecule force spectroscopy (SMFS). For more cells, see Figures S2a and S2b. (f) Box plot of binding probability for *S. aureus* cells with or without CCN1 preincubation measured by SMFS. $n$ = 12 and 13 cells, respectively. Stars indicate mean values, lines indicate medians, boxes indicate 25−75% quartiles, and whiskers indicate standard deviation. $P$ values were determined by a two-sample $t$ test in Origin. ***$P < 0.001$.

engagement of the phagocytic receptor $\alpha_V\beta_3$ integrin, CCN1 could eliminate apoptotic neutrophils during wound healing.[19]

Notably, CCN1 has also been demonstrated to function as an opsonin for clearance of Gram-positive bacteria by $\alpha_V\beta_3$ integrin-mediated phagocytosis. Acting as pattern recognition receptors (PRRs) on immune cells (such as dendritic cells, macrophages, and neutrophils), CCN1 recognizes specific molecules on the pathogen surface. Binding of CCN1 to the PG of *S. aureus* is mediated by both vWC and TSR domains.[16] This allows the pathogen to be bridged to macrophages (in the ECM of the tissue) and neutrophils (in the blood or at site of infection in the tissues) via their phagocytic receptor $\alpha_V\beta_3$ integrins. The primary binding site in soluble CCN1 for $\alpha_V\beta_3$ integrin has been localized in a 20-amino acid residue sequence within the vWC domain, whereas additional cryptic site(s) become exposed in the CT domain when CCN1 is surface-coated. This integrin-binding site does not contain the canonical RGD motif usually present in a number of ligands of $\alpha_V\beta_3$ integrin.[22] Importantly, a mutated CCN1 protein with a single residue substitution (Asp to Ala) within the vWC domain resulted defective for binding to $\alpha_V\beta_3$ integrin but was still able to bind PG,[22] suggesting that the CCN1 binding site(s) for *S. aureus* is distinct from those for integrin. Thus, CCN1 may function as a linker between PG and $\alpha_V\beta_3$ integrin, facilitating the formation of a ternary complex (PG−CCN1−$\alpha_V\beta_3$ integrin) that is compatible with its dual role depending on the target cells: (i) an opsonic complex for macrophages/neutrophils during phagocytosis; (ii) an adhesion system to non-phagocytic cells expressing $\alpha_V\beta_3$ integrin.

Despite the biological importance of the CCN1 bridge in the *S. aureus* phagocytosis, the mechanical forces driving this ternary interaction are unknown. Here, we address this issue using single-molecule force spectroscopy experiments. The results support a model in which CCN1 engages into two distinct force-dependent interaction mechanisms to enhance the mechanical stability of the PG−CCN1−$\alpha_V\beta_3$ integrin bridge, i.e., exposure and activation of cryptic integrin binding sites and multivalent binding of GlcNAc sugars by multiple lectin sites. This study rationalizes at the molecular level the ability of CCN1 to trigger *S. aureus* $\alpha_V\beta_3$ integrin-mediated


https://doi.org/10.1021/acs.nanolett.4c01533
Nano Lett. 2024, 24, 8567−8574

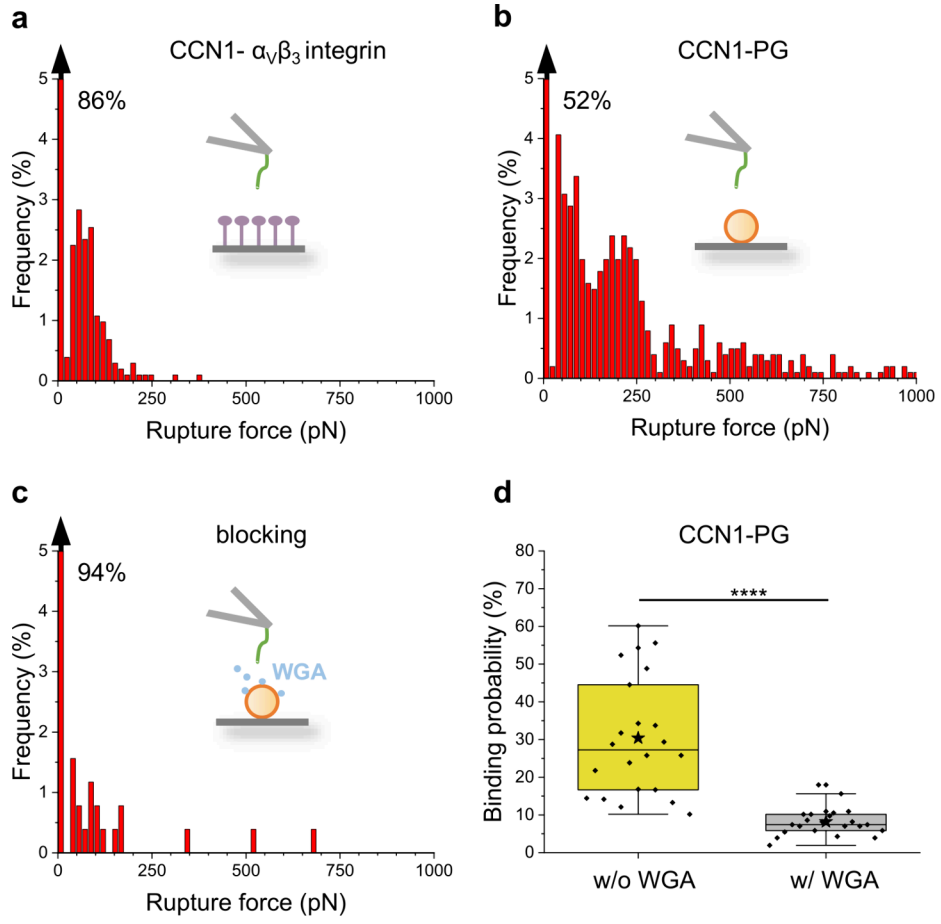


**Figure 2.** Mechanics and specificity of CCN1−$\alpha_V\beta_3$ integrin and CCN1−PG binary complexes. (a) Rupture force histogram showing the binding strength of the binary complex formed between CCN1 and $\alpha_V\beta_3$ integrin, as measured by SMFS. For more cells, see Figure S3a. (b, c) Rupture force histograms of representative *S. aureus* cells probed by SMFS with AFM tips functionalized with CCN1, before (b) and after (c) blocking with wheat germ agglutinin (WGA). For more cells, see Figures S3b and S3c, respectively. (d) Box plot showing the inhibitory effect of WGA (final concentration of 40 $\mu$g mL$^{-1}$) toward CCN1−PG interaction. $n$ = 22 cells (left box); $n$ = 23 cells (right box). Stars indicate mean values, lines indicate medians, boxes indicate 25−75% quartiles, and whiskers indicate standard deviation. $P$ values were determined by a two-sample $t$ test in Origin. ****$P$ < 0.0001.

adhesion and phagocytosis and shows promise for new effective therapies to enhance the immune response against this pathogen.

We first studied the mechanical strength of the interaction between CCN1, *S. aureus*, and $\alpha_V\beta_3$ integrin using single-cell force spectroscopy (SCFS; Figure 1). We used *S. aureus* Δ*srtA* cells which do not express cell wall-anchored proteins, in order to exclude the interference from surface proteins. A single live *S. aureus* bacterium preincubated or not with CCN1 was attached to a colloidal probe and then approached to a surface functionalized with $\alpha_V\beta_3$ integrins (Figure 1a,b). Force−distance curves were recorded, enabling us to estimate rupture force and binding probabilities. For CCN1-treated cells, a substantial number of force curves (average binding probability of 67%) featured adhesion (rupture) events with forces of 67 ± 14 pN (mean ± s.d., from a total of $n$ = 888 adhesive curves from 9 independent cells; Figure 1a,c and Figure S1a). The sharp maximum in the force distribution observed below 200 pN suggests that single bonds were probed with our SCFS experiments. By contrast, nontreated cells showed lower binding probability of 18% ($n$ = 7 different cells), providing direct evidence that CCN1 promotes *S. aureus* adhesion to $\alpha_V\beta_3$ integrin (Figure 1c).

Using single-molecule force spectroscopy (SMFS), we quantified the forces between single integrins immobilized on the AFM tip and *S. aureus* cells preincubated or not with CCN1 (Figure 1d,e). For treated bacteria, about 60% ($n$ = 12 independent cells) of the curves featured adhesion forces in the 25−500 pN range, with a clear maximum centered at 72 ± 20 pN (mean ± s.d., $n$ = 605 adhesive curves; 12 cells) that we attribute to single bonds. The remaining percentage of curves showed no adhesion events. These forces of single integrin and *S. aureus* preincubated with CCN1 are in line with our SCFS measurements and, importantly, agree with the strength of single integrins.[23−26] We note that SMFS histograms showed forces in the 200−400 pN range that were not observed in SCFS, which are likely to reflect the rupture of multiple bonds in parallel. We suggest that the reason this was not observed in SCFS is related to the complexity of the ternary interaction and to the very different geometries of the interacting surfaces. For instance, it is possible that integrins immobilized on a nanosize tip (SMFS) might be in a better geometry and molecular freedom to interact than when immobilized on a flat substrate (SCFS). Finally, adhesion was almost abolished for nontreated cells, with a decrease in binding probability from 60% to 4% ($n$ = 12 and 13 independent cells, respectively)


https://doi.org/10.1021/acs.nanolett.4c01533
Nano Lett. 2024, 24, 8567−8574

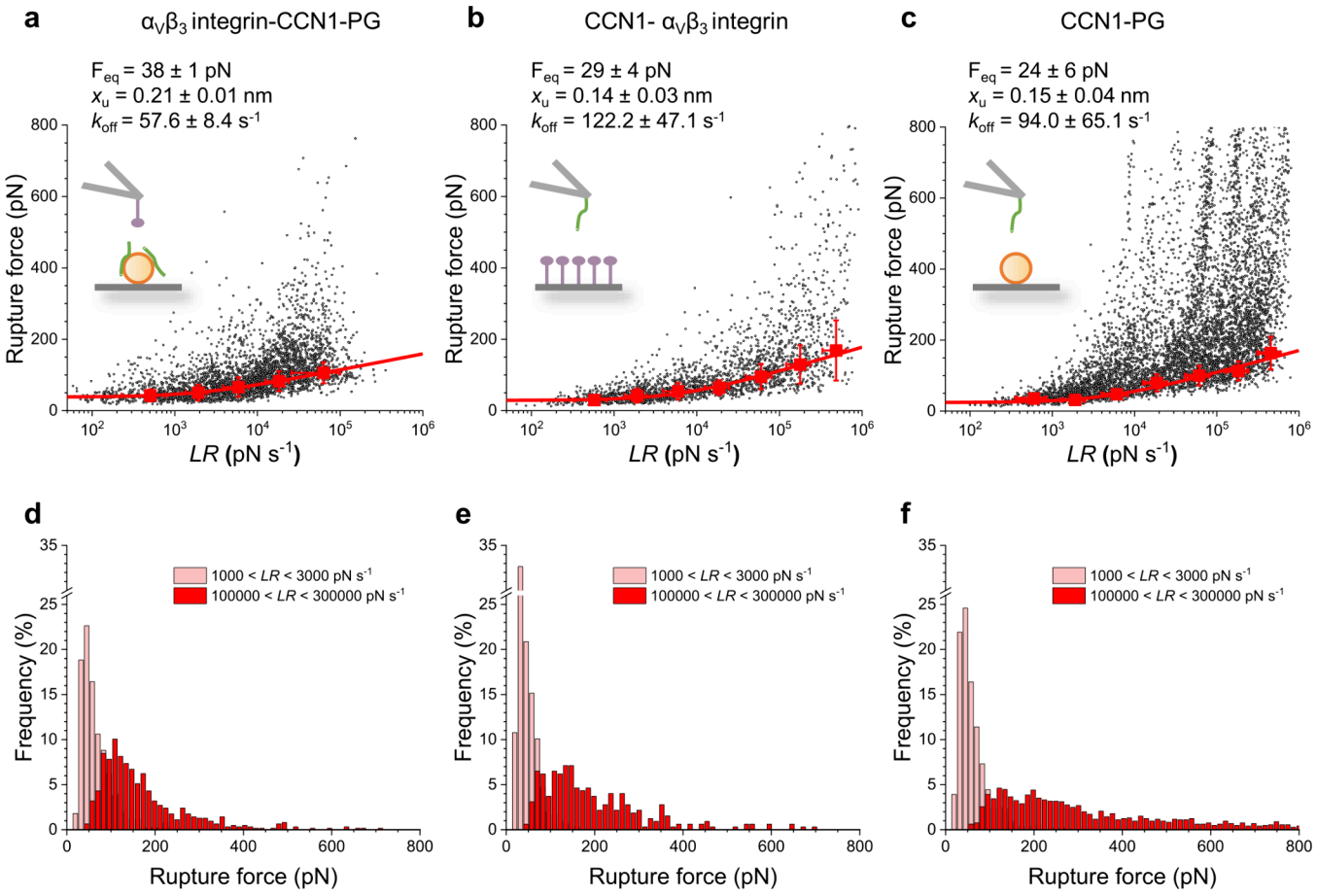


**Figure 3.** CCN1 ternary and binary complexes under mechanical tension. (a–c) Dynamic force spectroscopy plots (force, *F*, vs loading rate, *LR*) for the $\alpha_V\beta_3$ integrin–CCN1–PG ternary interaction (a), CCN1–$\alpha_V\beta_3$ integrin binary interaction (b), and CCN1–PG binary interaction (c). Fitting the data using the Friddle–Noy–de Yoreo model (lines) provided $F_{eq}$, $x_u$, and $k_{off}$ ($F_{eq}$) values with errors representing the s.d. Data were pooled from a total number of $n$ = 3280 adhesive curves for (a), $n$ = adhesive 6562 curves for (b), and $n$ = 2003 adhesive curves for (c). (d–f) Adhesion force histograms obtained by sorting the DFS data in discrete *LR* ranges for the different interactions.

(Figure 1f), leading us to conclude that CCN1 plays an essential role in establishing a mechanically strong bridge between *S. aureus* and $\alpha_V\beta_3$ integrin.

Then, we sought to unravel the relative contribution of each molecular partners to the mechanostability of the $\alpha_V\beta_3$ integrin–CCN1–PG complex. Given that in a ternary complex the weakest end is expected to rupture first, we measured the bond strength of CCN1–$\alpha_V\beta_3$ integrin and CCN1–PG binary interactions using single-molecule force spectroscopy. To this end, AFM tips functionalized with CCN1 were approached on surfaces functionalized with $\alpha_V\beta_3$ integrins or on top of a *S. aureus* cell immobilized on a substrate. Rupture force histograms (Figure 2a and Figure S3a) of multiple cells showed an average binding strength of 59 ± 9 pN ($n$ = 578 adhesive curves; 11 spots; 3 tips) for the CCN1–$\alpha_V\beta_3$ integrin binary complex, with an average binding probability around 17%. This force value falls within the 100 pN range of classical ligand–integrin bonds studied.[23−26] Remarkably, in the case of the CCN1–PG binary complex (Figure 2b and Figure S3b), force histograms displayed a wider distribution with stronger forces, from 50 to 800 pN (out of 2410 adhesive curves in total; 22 cells). The results indicate that the CCN1–PG bond is the strongest, i.e., that the CCN1–$\alpha_V\beta_3$ integrin bond of the ternary complex will rupture first under force.

To further characterize the CCN1–PG interaction and identify the bacterial component involved in it, wheat germ agglutinin (WGA), a lectin that recognizes the *N*-acetyl-glucosamine (GlcNAc) component of the polysaccharide moiety of PG, was injected into the system. As shown in Figure 2c,d, adhesion between CCN1 tips and the bacterial surface was significantly abrogated upon WGA addition, resulting in a sharp decrease of binding probability from 30% to 8% ($n$ = 22 and 23 different cells, respectively). This hints at GlcNAc of PG being the target ligand of CCN1. Knowing that both the vWC and TSP regions of CCN1 are able to bind PG and considering that up to three subsites within one carbohydrate-binding site of the WGA molecule were suggested for PG binding,[27] we speculate that the high forces (>100 pN) observed before WGA blocking result from multiple CCN1–PG interactions.

As the CCN1-mediated phagocytosis occurs under shear stress, we wondered how the ternary and binary complexes respond to mechanical force. In order to calculate the kinetic parameters describing the two binary complexes and further more compare them with the ternary complex, we assessed the dynamics of the interactions by measuring the adhesion forces ($F$) while varying the loading rate ($LR$), i.e., the rate at which force is applied (estimated from the force vs time curves). Dynamic force data (Figure 3) were obtained under different


https://doi.org/10.1021/acs.nanolett.4c01533
Nano Lett. 2024, 24, 8567−8574

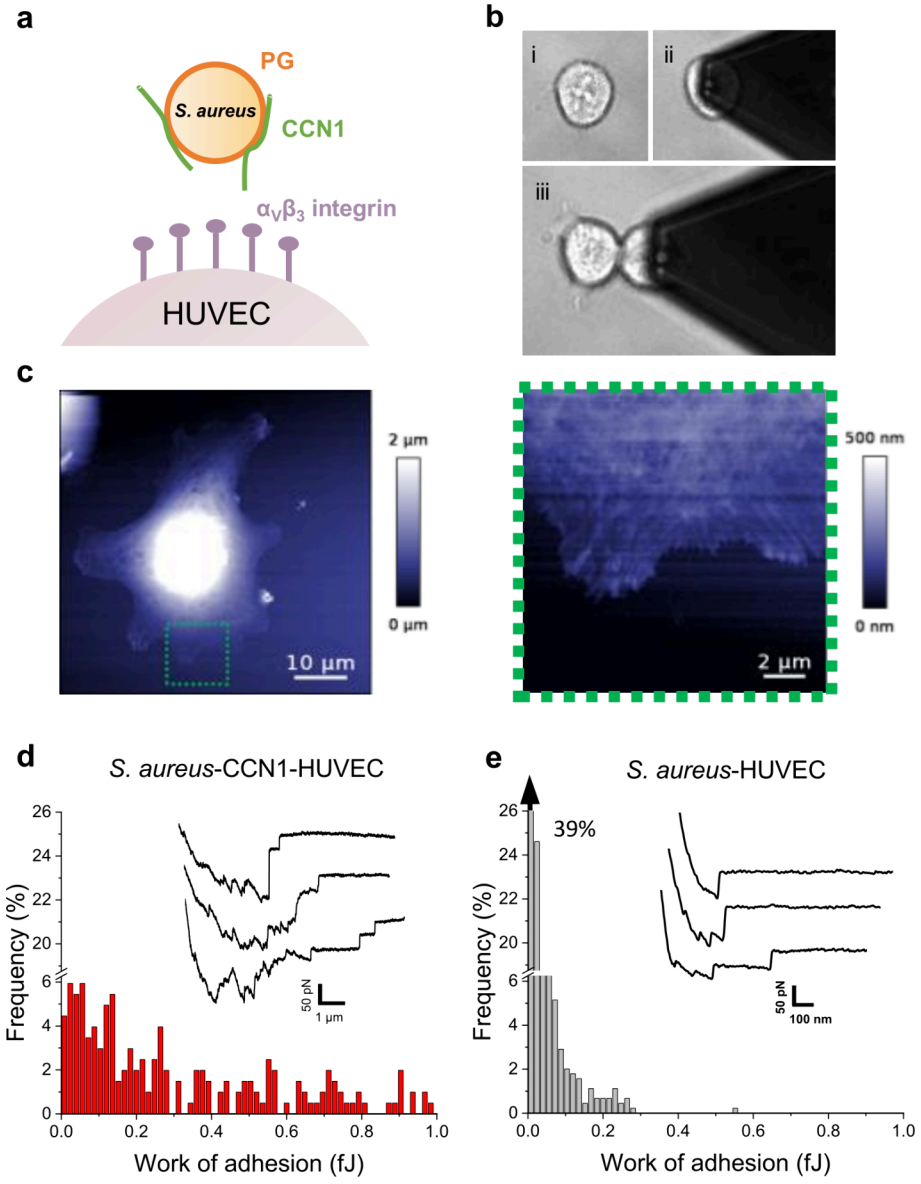


**Figure 4.** CCN1 functions as a mechanical bridge between *S. aureus* and host cells. (a) Scheme displaying the PG−CCN1−$\alpha_V\beta_3$ integrin ternary interaction. CCN1 molecules bind to the PG of *S. aureus* and act as a bridge promoting the interaction between *S. aureus* and integrins exposed on the surface of human umbilical vein endothelial cells (HUVECs). (b) Optical images (40× resolution) showing a HUVEC probed by MSCT-C cantilever in HEPES buffer. (i) To promote the exposure of $\alpha_V\beta_3$ integrins in the upper cell membrane, HUVECs were trypsinized to remove ECM proteins and immobilized on glass substrates coated with ConA lectins. (ii, iii) One HUVEC cell dividing into two cells during the experiments demonstrated the viability of the cell. (c) Height images of a HUVEC probed by MSCT-C cantilever using the multiparametric AFM imaging mode. Left: image of a full isolated cell; right: zoomed-in image of the same cell. (d) Histogram showing the work of adhesion, obtained in HEPES between *S. aureus* bacterial probes preincubated with CCN1 and HUVECs exposing integrins in their upper membrane. Eight different cell pairs of 216 adhesive curves merged. Inset representative adhesion force profiles with multiple peaks and plateaus. These force events were followed by discrete jumps reflecting rupture of intermolecular bonds. The force plateaus indicate extraction of cytoskeleton-free membrane tubes (tethers) from the cell membrane during measurements. (e) Data for control experiments in which *S. aureus* cells were not preincubated with CCN1. Ten different cell pairs of 447 adhesive curves merged. Insets: representative retraction profiles.

pulling speeds ranging from 0.5 to 10 $\mu$m $s^{-1}$ for $\alpha_V\beta_3$ integrin−CCN1−PG (Figure 3a), CCN1−$\alpha_V\beta_3$ integrin (Figure 3b), and CCN1−PG (Figure 3c) complexes. Data corresponding to single interactions were fitted with the Friddle−Noy−de Yoreo model,[28] yielding $F_{eq}$ (the equilibrium force), $x_u$ (distance from the bound state to the transition state barrier), and $k_{off}$ (dissociation rate at the equilibrium force) values. The three systems featured rather similar kinetics parameters ($k_{off}$ = 57.6 ± 8.4 $s^{-1}$ for the ternary complex, compared with $k_{off}$ = 122.2 ± 47.1 $s^{-1}$ for the CCN1−$\alpha_V\beta_3$ integrin binary complex and $k_{off}$ = 94.0 ± 65.1 $s^{-1}$ for the CCN1−PG binary complex). The high $k_{off}$ values illustrate the high dissociation rates of the complexes compared to some staphylococcal adhesins.[29−32]

DFS plots clearly indicated that the interactions become stronger at increasing *LR*s. We therefore dissected the distribution of ruptures forces over discrete ranges of *LR*s (Figure 3d−f). The probability of forming strong adhesion increased with the *LR*, well beyond the values expected for single bonds, implying that the CCN1 interactions strengthen


https://doi.org/10.1021/acs.nanolett.4c01533
Nano Lett. 2024, 24, 8567−8574

with the applied force. At high loading rates, the CCN1−$\alpha_V\beta_3$ integrin and the ternary complexes behaved similarly: at lowest *LRs* (<3000 pN/s) they showed mostly weak forces centered at 39 ± 17 pN ($n$ = adhesive 297 curves, 3 spots) and 50 ± 20 pN ($n$ = 499 adhesive curves, 4 cells), while at the highest *LRs* (>100000 pN/s) they featured higher forces of 117 ± 44 pN ($n$ = 326 adhesive curves, 3 spots) and 124 ± 48 pN ($n$ = adhesive 627 curves, 4 cells). For both systems, we argue that the low forces result from single (perhaps multiple) bonds between the primary $\alpha_V\beta_3$ integrin binding site in the CCN1 vWC domain, whereas under increasing tensile load, additional cryptic site(s) in the CCN1 CT domain become exposed and available for interaction with $\alpha_V\beta_3$ integrin.[25]

By contrast, the CCN1−PG complex at the high *LRs* (>100000 pN/s) featured forces up to 800 pN, emphasizing again that the latest is the strongest link of the bridge. We speculate that strong forces arise from multivalent binding, i.e., the simultaneous rupture of multiple bonds between CCN1 and GlcNAc of PG. This is supported by the notion that both the vWC and TSP regions have lectin sites that bind PG and that lectins like WGA can have multiple subsites within one carbohydrate-binding site.[27] Indeed, WGA exhibited multivalent binding by forming dimers and simultaneously providing eight sugar binding sites for GlcNAc.[33] We note that the DFS data for the CCN1−PG complex could not be fitted with the Williams−Evans prediction for multiple bonds (Figure S4).[34] This indicates that we are not in the presence of uncorrelated interactions occurring in parallel but that some other phenomenon like cooperative binding between lateral ligands must occur.

Finally, we asked whether CCN1 is capable to tightly bridge *S. aureus* and living host cells, using human endothelial cells (HUVEC) as a non-phagocytic cell line expressing $\alpha_V\beta_3$ integrins. To promote the exposure of $\alpha_v\beta_3$ integrins in the upper cell membrane, cells were trypsinized to remove ECM proteins and further immobilized on glass substrates coated with lectins for analysis.[24,35] Then, we measured the forces between *S. aureus* with or without CCN1 preincubation and HUVECs. SCFS experiments between CCN1-treated *S. aureus* bacteria and endothelial cells featured complex adhesion force profiles with multiple peaks and plateaus (insets in Figure 4d). These force events were followed by discrete jumps reflecting rupture of intermolecular bonds. The force plateaus indicate extraction of cytoskeleton-free membrane tubes (tethers) from the cell membrane during measurements.[36,37] Membrane tethers may help enhancing the duration of *S. aureus*−host cell adhesive contacts during phagocytosis. Unlike discrete adhesive events, the work that is required to detach the cell can be used to describe the adhesion strength of the cell. We therefore estimated the work of adhesion ($W_{adh}$) by considering the area under the retraction curves. As shown in Figure 4d, large $W_{adh}$ values (up to 1 fJ) were observed for treated bacteria, which indicates that the soft, deformable host membrane partly covers the bacterial cell surface, thus highlighting the role of membrane deformation in determining the energy and duration of bacterial-host adhesion. $W_{adh}$ values were dramatically reduced for nontreated *S. aureus* bacteria (Figure 4e), confirming the essential role of CCN1 in enhancing *S. aureus* adhesion to human host cells and validating the above results on purified integrins.

In summary, this study sheds new light into the mechanism of CCN1-mediated adhesion and phagocytosis by providing molecular insights into the mechanics of the ternary bridge between CCN1, bacterial PG, and host cell integrins. Phagocytosis is an important mechanism of the immune system where pathogens are engulfed and further eliminated by immune cells like macrophages and neutrophils. Understanding the molecular basis of CCN1-mediated *S. aureus* phagocytosis offers prospects for the design of new therapeutics to boost the immune response against this pathogen. The main finding of our work is that CCN1 behaves as a force-sensitive linker that potentiates staphylococcal adhesion under mechanical stress. The strengths of the CCN1−PG and CCN1−$\alpha_V\beta_3$ integrin binary interactions are weak (moderate) at low tensile force but are dramatically enhanced by mechanical tension. Our results support a model in which CCN1 engages into two distinct force-dependent interaction mechanisms to enhance its mechanical stability as a molecular bridge. On the one hand, mechanical force induces unfolding of the CCN1 CT domain, causing the exposure of cryptic integrin-binding sites, which in turn engages into a high affinity interaction with the integrins.[38] This mechanical response is reminiscent of the three-component FnBPA−Fn−$\alpha_5\beta_1$ complex, whereby upon binding of Fn to FnBPA, force-induced unfold FnIII domains, causing the exposure of high affinity, buried integrin-binding sites.[35] On the other hand, multivalent binding of GlcNAc sugars by lectin sites is favored under mechanical tension. Multivalent binding is used by some bacterial pathogens to enhance adhesion, the prototypical example being the adhesion of *Escherichia coli*.[39] The affinity of carbohydrates for bacterial lectins is low, but presentation of multiple copies of carbohydrates leads to high-affinity multivalent binding.[40−42] Multivalent binding interactions have increased avidity compared to monovalent ones as their off rate is much slower. The reason for this is that there is a high chance that sugar ligands rebind before complete dissociation of the complex due to their high local concentration. Multivalency is clearly expected as the target GlcNAc sugars are present at high density along the PG chains and as both the vWC and TSP regions of CCN1 have lectin sites. Importantly, the GlcNAc lectin WGA has several binding sites per subunit that are distributed over the whole protein, meaning that WGA dimers accommodate eight independent binding sites.[33] Therefore, we expect that adjacent protein−carbohydrate bonds will strongly favor and enhance high-affinity interactions.

## ■ ASSOCIATED CONTENT

### Supporting Information

The Supporting Information is available free of charge at https://pubs.acs.org/doi/10.1021/acs.nanolett.4c01533.

Detailed information about methods; Figure S1: SCFS rupture force histograms obtained by probing $\alpha_V\beta_3$ integrin-functionalized surfaces with single *S. aureus* cells treated (a) or not (b) with CCN1; Figure S2: SMFS rupture force histograms of single *S. aureus* cells treated (a) or not (b) with CCN1, probed with AFM tips functionalized with $\alpha_V\beta_3$ integrin; Figure S3: mechanical strength of CCN1−$\alpha_V\beta_3$ integrin and CCN1−PG binary complexes; Figure S4: CCN1−PG binary complex binding dynamics; Williams−Evans fit for multiple bonds (DOCX)



https://doi.org/10.1021/acs.nanolett.4c01533
Nano Lett. 2024, 24, 8567−8574

## AUTHOR INFORMATION


### Corresponding Authors

**Yves F. Dufrêne** − *Louvain Institute of Biomolecular Science and Technology, UCLouvain, B-1348 Louvain-la-Neuve, Belgium*; orcid.org/0000-0002-7289-4248; Email: yves.dufrene@uclouvain.be

**Pietro Speziale** − *Department of Molecular Medicine, Biochemistry Unit, University of Pavia, 27100 Pavia, Italy*; Email: pietro.speziale@unipv.it

### Authors

**Can Wang** − *Louvain Institute of Biomolecular Science and Technology, UCLouvain, B-1348 Louvain-la-Neuve, Belgium*

**Telmo O. Paiva** − *Louvain Institute of Biomolecular Science and Technology, UCLouvain, B-1348 Louvain-la-Neuve, Belgium*

Complete contact information is available at: https://pubs.acs.org/10.1021/acs.nanolett.4c01533


### Author Contributions

C.W., P.S., and Y.F.D. designed the experiments. C.W. performed the experiments as well as collected and analyzed the data. T.O.P. assisted with data analysis. C.W., T.O.P., P.S, and Y.F.D. wrote the article.

### Notes

The authors declare no competing financial interest.

## ACKNOWLEDGMENTS

Work at the Université catholique de Louvain was supported by the National Fund for Scientific Research (FNRS). Y.F.D. is a Research Director at the FNRS.

## REFERENCES


(1) Cheung, G. Y. C.; Bae, J. S.; Otto, M. Pathogenicity and Virulence of *Staphylococcus aureus*. *Virulence* **2021**, *12* (1), 547−569.

(2) Foster, T. J.; Geoghegan, J. A.; Ganesh, V. K.; Höök, M. Adhesion, Invasion and Evasion: the Many Functions of the Surface Proteins of *Staphylococcus aureus*. *Nat. Rev. Microbiol.* **2014**, *12* (1), 49−62.

(3) Visansirikul, S.; Kolodziej, S. A.; Demchenko, A. V. *Staphylococcus aureus* Capsular Polysaccharides: a Structural and Synthetic Perspective. *Org. Biomol Chem.* **2020**, *18* (5), 783−798.

(4) Mohammad, M.; Ali, A.; Nguyen, M.-T.; Götz, F.; Pullerits, R.; Jin, T. *Staphylococcus aureus* Lipoproteins in Infectious Diseases. *Front. Microbiol.* **2022**, *13*, 1006765.

(5) Tam, K.; Torres, V. J. *Staphylococcus aureus* Secreted Toxins & Extracellular Enzymes. *Microbiol. Spectr.* **2019**, *7* (2), GPP3-0039-2018.

(6) Sharif, S.; Singh, M.; Kim, S. J.; Schaefer, J. *Staphylococcus aureus* Peptidoglycan Tertiary Structure from Carbon-13 Spin Diffusion. *J. Am. Chem. Soc.* **2009**, *131* (20), 7023−7030.

(7) Kim, S. J.; Chang, J.; Singh, M. Peptidoglycan Architecture of Gram-Positive Bacteria by Solid-State NMR. *Biochim. Biophys. Acta* **2015**, *1848* (0), 350−362.

(8) Fournier, B.; Philpott, D. J. Recognition of *Staphylococcus aureus* by the Innate Immune System. *Clin. Microbiol. Rev.* **2005**, *18* (3), 521−540.

(9) Maršavelski, A.; Paurević, M.; Ribić, R. Mannosylated Adamantane-Containing Desmuramyl Peptide Recognition by the NOD2 Receptor: a Molecular Dynamics Study. *Org. Biomol Chem.* **2021**, *19* (32), 7001−7012.

(10) Iwaki, D.; Mitsuzawa, H.; Murakami, S.; Sano, H.; Konishi, M.; Akino, T.; Kuroki, Y. The Extracellular Toll-like Receptor 2 Domain Directly Binds Peptidoglycan Derived from *Staphylococcus aureus*. *J. Biol. Chem.* **2002**, *277* (27), 24315−24320.

(11) Dziarski, R.; Kashyap, D. R.; Gupta, D. Mammalian Peptidoglycan Recognition Proteins Kill Bacteria by Activating Two-Component Systems and Modulate Microbiome and Inflammation. *Microb Drug Resist* **2012**, *18* (3), 280−285.

(12) Jun, J.-I.; Lau, L. F. Taking Aim at the Extracellular Matrix: CCN Proteins as Emerging Therapeutic Targets. *Nat. Rev. Drug Discovery* **2011**, *10* (12), 945−963.

(13) Lau, L. F. CCN1/CYR61: The Very Model of a Modern Matricellular Protein. *Cell. Mol. Life Sci.* **2011**, *68* (19), 3149−3163.

(14) Lau, L. F. Cell Surface Receptors for CCN Proteins. *J. Cell Commun. Signal* **2016**, *10* (2), 121−127.

(15) Lau, L. F.; Lam, S. C.-T. The CCN Family of Angiogenic Regulators: the Integrin Connection. *Exp. Cell Res.* **1999**, *248* (1), 44−57.

(16) Jun, J.-I.; Lau, L. F. CCN1 Is an Opsonin for Bacterial Clearance and a Direct Activator of Toll-like Receptor Signaling. *Nat. Commun.* **2020**, *11* (1), 1242.

(17) Choi, J. S.; Kim, K.-H.; Lau, L. F. The Matricellular Protein CCN1 Promotes Mucosal Healing in Murine Colitis through IL-6. *Mucosal Immunol* **2015**, *8* (6), 1285−1296.

(18) Kim, K.-H.; Chen, C.-C.; Alpini, G.; Lau, L. F. CCN1 Induces Hepatic Ductular Reaction through Integrin $\alpha_v\beta_5$-Mediated Activation of NF-κB. *J. Clin Invest* **2015**, *125* (5), 1886−1900.

(19) Jun, J.-I.; Kim, K.-H.; Lau, L. F. The Matricellular Protein CCN1Mediates Neutrophil Efferocytosis in Cutaneous Wound Healing. *Nat. Commun.* **2015**, *6* (1), 7386.

(20) Wells, J. E.; Howlett, M.; Cheung, L. C.; Kees, U. R. The Role of CCN Family Genes in Haematological Malignancies. *J. Cell Commun. Signal.* **2015**, *9* (3), 267−278.

(21) Chen, C.-C.; Mo, F.-E.; Lau, L. F. The Angiogenic Factor Cyr61 Activates a Genetic Program for Wound Healing in Human Skin Fibroblasts. *J. Biol. Chem.* **2001**, *276* (50), 47329−47337.

(22) Chen, N.; Leu, S.-J.; Todorović, V.; Lam, S. C.-T.; Lau, L. F. Identification of a Novel Integrin $\alpha_V\beta_3$ Binding Site in CCN1 (CYR61) Critical for Pro-Angiogenic Activities in Vascular Endothelial Cells. *J. Bio. Chem.* **2004**, *279* (42), 44166−44176.

(23) Li, F.; Redick, S. D.; Erickson, H. P.; Moy, V. T. Force Measurements of the $\alpha_5\beta_1$ Integrin-Fibronectin Interaction. *Biophys. J.* **2003**, *84* (2), 1252−1262.

(24) Bharadwaj, M.; Strohmeyer, N.; Colo, G. P.; Helenius, J.; Beerenwinkel, N.; Schiller, H. B.; Fässler, R.; Müller, D. J. αV-Class Integrins Exert Dual Roles on α5β1 Integrins to Strengthen Adhesion to Fibronectin. *Nat. Commun.* **2017**, *8* (1), 14348.

(25) Viela, F.; Speziale, P.; Pietrocola, G.; Dufrêne, Y. F. Mechanostability of the Fibrinogen Bridge between Staphylococcal Surface Protein ClfA and Endothelial Cell Integrin $\alpha_V\beta_3$. *Nano Lett.* **2019**, *19* (10), 7400−7410.

(26) Mathelié-Guinlet, M.; Viela, F.; Alfeo, M. J.; Pietrocola, G.; Speziale, P.; Dufrêne, Y. F. Single-Molecule Analysis Demonstrates Stress-Enhanced Binding between *Staphylococcus aureus* Surface Protein IsdB and Host Cell Integrins. *Nano Lett.* **2020**, *20* (12), 8919−8925.

(27) Lienemann, M.; Paananen, A.; Boer, H.; de la Fuente, J. M.; García, I.; Penadés, S.; Koivula, A. Characterization of the Wheat Germ Agglutinin Binding to Self-Assembled Monolayers of Neoglycoconjugates by AFM and SPR. *Glycobiology* **2009**, *19* (6), 633−643.

(28) Friddle, R. W.; Noy, A.; De Yoreo, J. J. Interpreting the Widespread Nonlinear Force Spectra of Intermolecular Bonds. *Proc. Natl. Acad. Sci. U. S. A.* **2012**, *109* (34), 13573−13578.

(29) Herman, P.; El-Kirat-Chatel, S.; Beaussart, A.; Geoghegan, J. A.; Foster, T. J.; Dufrêne, Y. F. The Binding Force of the Staphylococcal Adhesin SdrG Is Remarkably Strong. *Mol. Microbiol.* **2014**, *93* (2), 356−368.

(30) Milles, L. F.; Schulten, K.; Gaub, H. E.; Bernardi, R. C. Molecular Mechanism of Extreme Mechanostability in a Pathogen Adhesin. *Science* **2018**, *359* (6383), 1527−1533.

(31) Wang, C.; Chantraine, C.; Viljoen, A.; Herr, A. B.; Fey, P. D.; Horswill, A. R.; Mathelié-Guinlet, M.; Dufrêne, Y. F. The Staph-

ylococcal Biofilm Protein Aap Mediates Cell-Cell Adhesion through Mechanically Distinct Homophilic and Lectin Interactions. *PNAS Nexus* **2022**, *1* (5), pgac278.
(32) Wang, C.; Paiva, T. O.; Motta, C.; Speziale, P.; Pietrocola, G.; Dufrêne, Y. F. Catch Bond-Mediated Adhesion Drives *Staphylococcus aureus* Host Cell Invasion. *Nano Lett.* **2023**, *23* (11), 5297−5306.
(33) Schwefel, D.; Maierhofer, C.; Beck, J. G.; Seeberger, S.; Diederichs, K.; Möller, H. M.; Welte, W.; Wittmann, V. Structural Basis of Multivalent Binding to Wheat Germ Agglutinin. *J. Am. Chem. Soc.* **2010**, *132* (25), 8704−8719.
(34) Alsteens, D.; Pfreundschuh, M.; Zhang, C.; Spoerri, P. M.; Coughlin, S. R.; Kobilka, B. K.; Müller, D. J. Imaging G Protein-Coupled Receptors While Quantifying Their Ligand-Binding Free-Energy Landscape. *Nat. Methods* **2015**, *12* (9), 845−851.
(35) Prystopiuk, V.; Feuillie, C.; Herman-Bausier, P.; Viela, F.; Alsteens, D.; Pietrocola, G.; Speziale, P.; Dufrêne, Y. F. Mechanical Forces Guiding *Staphylococcus aureus* Cellular Invasion. *ACS Nano* **2018**, *12* (4), 3609−3622.
(36) Franz, C. M.; Taubenberger, A.; Puech, P.-H.; Muller, D. J. Studying Integrin-Mediated Cell Adhesion at the Single-Molecule Level Using AFM Force Spectroscopy. *Science's STKE* **2007**, *2007* (406), pl5.
(37) Helenius, J.; Heisenberg, C.-P.; Gaub, H. E.; Muller, D. J. Single-Cell Force Spectroscopy. *J. Cell Sci.* **2008**, *121* (11), 1785−1791.
(38) Liang, X.; Garcia, B. L.; Visai, L.; Prabhakaran, S.; Meenan, N. A. G.; Potts, J. R.; Humphries, M. J.; Höök, M. Allosteric Regulation of Fibronectin/$\alpha_5\beta_1$ Interaction by Fibronectin-Binding MSCRAMMs. *PLoS One* **2016**, *11* (7), No. e0159118.
(39) Beaussart, A.; Abellan-Flos, M.; El-Kirat-Chatel, S.; Vincent, S. P.; Dufrene, Y. F. Force Nanoscopy as a Versatile Platform for Quantifying the Activity of Antiadhesion Compounds Targeting Bacterial Pathogens. *Nano. Lett.* **2016**, *16* (2), 1299−1307.
(40) Lindhorst, T. K.; Kieburg, C.; Krallmann-Wenzel, U. Inhibition of the Type 1 Fimbriae-Mediated Adhesion of *Escherichia Coli* to Erythrocytes by Multiantennary $\alpha$-Mannosyl Clusters: the Effect of Multivalency. *Glycoconj. J.* **1998**, *15* (6), 605−613.
(41) Lindhorst, T. K.; Dubber, M. Octopus Glycosides: Multivalent Molecular Platforms for Testing Carbohydrate Recognition and Bacterial Adhesion. *Carbohydr. Res.* **2015**, *403*, 90−97.
(42) Bhatia, S.; Camacho, L. C.; Haag, R. Pathogen Inhibition by Multivalent Ligand Architectures. *J. Am. Chem. Soc.* **2016**, *138* (28), 8654−8666.


https://doi.org/10.1021/acs.nanolett.4c01533
*Nano Lett.* 2024, 24, 8567−8574